



Molecular classification of benign prostatic hyperplasia: A gene expression profiling study in a rat model

| | |
|-------|---|
| メタデータ | 言語: English 出版者: 公開日: 2019-06-21 キーワード (Ja): キーワード (En): 作成者: 秦, 淳也 メールアドレス: 所属: |
| URL | https://fmu.repo.nii.ac.jp/records/2000190 |

(表紙記載例)

学 位 論 文

学位論文名

Molecular classification of benign prostatic hyperplasia: A
gene expression profiling study in a rat model

(新規前立腺肥大症モデルラットを用いた遺伝子発現

プロファイリングによる前立腺肥大症の病態解明)

※論文名が英文の場合は、日本語訳を () 内に付記すること。

福島県立医科大学大学院医学研究科

泌尿器外科学分野

泌尿器科学講座

秦 淳也

論文概要

前立腺肥大症とは、前立腺が腫大することで、排尿困難、頻尿等の下部尿路症状をきたし、著しく患者の QOL を損なう疾患である。現在では、 α_1 遮断薬や 5α 還元酵素阻害薬といった内服薬で治療することが多い。しかしながら、それら内服薬に抵抗性の前立腺肥大症例も存在し、新たな標的分子の発見・新薬の開発が望まれている疾患の一つである。そこで今回、前立腺肥大症の発症機序を明らかにするために、新規に樹立した前立腺肥大症モデルラットを用いて網羅的遺伝子発現解析を行なった。まず、妊娠ラットから摘出した胎仔ラットより、尿生殖洞のみを単離し、7 週齢雄性ラットの腹側前立腺被膜下に移植することで、前立腺肥大症モデルラットを作成した。この方法で移植された尿生殖洞は、間質成分優位の組織像を呈し、ヒト前立腺肥大症と非常に類似した組織構造を示すことが特徴である。この前立腺肥大症組織を用いて、網羅的遺伝子発現機能解析を行なった。その結果、前立腺肥大症組織では、926 の特異的遺伝子の発現亢進、3,217 の特異的遺伝子の発現減弱がそれぞれ認められた。前立腺肥大症特異的遺伝子について、Gene Ontology 解析を行なったところ、development、response to stimulus、growth のカテゴリの遺伝子群と関連が

あった。さらに、**Functional network** 解析を行なったところ、アポトーシス経路、IL-2 情報伝達経路、IL-5 情報伝達経路、KIT 情報伝達経路、補体経路、B-cell 情報伝達経路、p38MAPK 経路等が活性化していた。一方、コレステロール合成経路の不活性化が認められた。以上の結果は、前立腺肥大症発症機序の解明の一助となる可能性がある。これらの分子機構を明らかにすることで、前立腺肥大症の新規標的分子の発見、ひいては新規治療薬の開発につながることを考えられた。

Gene expression profiling for molecular classification of benign prostatic hyperplasia rat model

Junya Hata, Yuichi Satoh, Hidenori Akaihata, Hiroyuki Hiraki, Soichiro Ogawa,

Nobuhiro Haga, Kei Ishibashi, Ken Aikawa, Yoshiyuki Kojima

Department of Urology, Fukushima Medical University School of Medicine,

Fukushima, Japan

Running head: Gene expression profiling of BPH rat model

Word count: Abstract: 246, Text: 2,995

Department of Urology, Fukushima Medical University School of Medicine

1 Hikarigaoka, Fukushima 960-1295, Japan

Tel.: +81-24-547-1316; Fax: +81-24-548-3393

E-mail: akju826@fmu.ac.jp

Abstract

Objectives: We performed gene expression profiling analysis using an experimental BPH rat model, which resembles human BPH pathology, to characterize the molecular features of BPH.

Methods: Fetal urogenital sinus (UGS) isolated from 20-day-old male rat embryo was implanted into a pubertal male rat ventral prostate. The implanted UGS grew time-dependently, and the pathological findings at 3 weeks after implantation showed epithelial hyperplasia as well as stromal hyperplasia. Whole-genome oligonucleotide microarray analysis utilizing approximately 30,000 oligonucleotide probes was performed using prostate specimens during the prostate growth process (3 weeks after implantation).

Results: Microarray analyses revealed 926 up-regulated (>2 -fold change, $p < 0.01$) and 3,217 down-regulated genes (<0.5 -fold change, $p < 0.01$) in BPH specimens compared with normal prostate. Gene ontology analyses of up-regulated genes revealed predominant genetic themes of involvement in development (162 genes, $p = 2.01 \times 10^{-4}$), response to stimulus (163 genes, $p = 7.37 \times 10^{-13}$) and growth (32 genes, $p = 1.93 \times 10^{-5}$).

When we used both normal prostate and non-transplanted UGSs as controls to identify BPH-specific genes, 507 and 406 genes were up-regulated and down-regulated, respectively. Functional network and pathway analyses showed that genes associated with apoptosis modulation by heat shock protein 70, IL-1, -2 and -5 signaling pathways, KIT signaling pathway, and secretin-like G-protein-coupled receptors, Class B, were relatively activated during the growth process in the BPH specimens. On the other hand, genes associated with cholesterol biosynthesis were relatively inactivated.

Conclusion: Our microarray analyses of the BPH model rat may be useful of clarifying the molecular mechanism of BPH progression and identify molecular targets for BPH treatment.

Key words: benign prostatic hyperplasia, growth, microarray, model, rat

Introduction

Benign prostatic hyperplasia (BPH) involves histologic changes of stromal and epithelial hyperplasia within discrete nodules that are generally located in the transition zone of the prostate [1,2]. Despite the spectacular new drug development and surgical successes achieved, the cellular and molecular processes underlying the pathogenesis and development of BPH remain poorly understood. Since we usually encounter patients with histologically developed BPH, it is difficult to investigate the prostate growth process in human BPH; therefore, there has been a need for a BPH animal model to provide us with molecular biological information and contribute to the identification of factors responsible for BPH.

The main components of human BPH specimens are smooth muscle, a fibrous tissue element and collagen, which are the major components of the stromal extracellular matrix [3]. Histologically, prostate specimens of normal rodents are epithelial component-dominant. There are several BPH model rats, including testosterone-induced model rats and spontaneously hypertensive rats [4,5]. The histological characteristic of the testosterone-induced model rats is that they are epithelial component dominant

prostate specimens that are associated with ductal enlargement and epithelial dysplasia [6]. Spontaneously hypertensive rats (SHRs) exhibit features of glandular hyperplasia of the ventral prostate, including the narrowing of acini with epithelial protrusions into the lumen and the piling up of epithelial cells [4,7,8]. They are fairly different from human BPH, the pathological findings of which show both epithelial and stromal hyperplasia. Therefore, these models may not necessarily be suitable as BPH rat models to elucidate the molecular and cellular mechanisms involved, and the establishment of a rodent model that exactly reproduces the histopathological appearance of human BPH has been anticipated. Recently, a rat model of BPH produced by implanting fetal urogenital sinus (UGS) into adult rat ventral prostate was developed [6,9,10]. This rat model, which has the characteristics of having epithelial and stromal hyperplasia and resembling human BPH pathology, was produced based on the theory of embryonic reawakening in the pathogenesis of BPH [11]. Therefore, we considered that this BPH model rat may be useful to clarify the development and pathogenesis of BPH.

In this study, in order to identify genes associated with the pathogenesis of BPH, we performed whole-genome oligonucleotide microarray analysis using the BPH model rat.

We also classified the expression of the differentially expressed genes by gene ontology analysis as well as functional network and pathway analysis in order to characterize the molecular features of BPH, and provide a guide to clarify the pathogenesis of BPH.

Methods

Experimental animals

We used a previously established experimental BPH model rat with pathologically stromal component-dominant hyperplasia (Fig. 1) [6,9,10]. Pregnant female rats that were at 20 days of pregnancy and 7-week-old male Sprague-Dawley (S-D) rats (Charles River Japan, Kanagawa, Japan) were used to produce a BPH model rat. First, we isolated 20-day-old male rat embryos from pregnant female rats. Second, the UGS was excised from the 20-day-old male rat embryos using a stereomicroscope. The trimmed UGS was washed with RPMI 1640 containing 10% fetal bovine serum and 1% penicillin/streptomycin. Third, the isolated UGS was implanted under the right ventral prostate capsule of 7-week-old adult male rats. After the host rats had been sacrificed 21 days after UGS implantation, the right ventral prostate was dissected free of connective

tissue. The implanted UGS, initially weighing approximately 1 mg, grew time-dependently, being more than 100 mg at 21 days after implantation, as previously reported [6,9,10]. The study was performed in accordance with the Guidelines for the Care and Use of Experimental Animals and protocols approved by the Animal Care Committee of Fukushima Medical University (#26020).

Total RNA isolation

Total RNA samples were isolated from implanted UGS harvested 21 days after implantation and the left ventral prostate (normal prostate) tissue of the same individual as a control with the RNeasy Midi Kit (Qiagen) in accordance with the manufacturer's instructions. Samples in three groups of normal prostate (n=4), non-transplanted UGS (n=40) and transplanted UGS (BPH specimens; n=4) were used in this study.

cRNA preparation and microarray analysis

The cRNA preparation and microarray analysis were conducted at Bio Matrix Research (Chiba, Japan) using the Affymetrix system (Santa Clara, CA, USA). One

microgram of total RNA was converted into stranded cDNA using the One-Cycle cDNA Synthesis Kit. In vitro transcription reactions were performed using a GeneChip IVT Labeling Kit. After purification of biotin-labeled cRNA using GeneChip Sample Cleanup Module, the concentration of cRNA was measured, and then 15 µg of cRNA was fragmented in the presence of a fragmentation buffer. The 15 µg of cRNA was hybridized using the GeneChip Rat Genome 230 2.0 array on the GeneChip Hybridization Oven. After hybridization, the array was washed and stained with the GeneChip on the GeneChip Fluidics Station, and finally the array was scanned using the GeneChip Scanner 3000 7G to detect each signal. Candidate mRNAs showing differential expression were identified using the Affymetrix GeneChip Rat Genome 230 2.0 array in accordance with the manufacturer's instructions. Eleven probe pairs, each of which consisted of perfect match and mismatch probes with 25-mers of oligonucleotide, were prepared per transcript. The mismatch was designed as a single-base substitute for the perfect match probe, which had a sequence complementary to the target transcript.

Microarray data analysis

The expression value of the transcript was computed using GeneChip Operating Software. Normalization, relative signal intensities and fold changes among normal prostate, UGS and BPH specimens were calculated using Gene Spring[®] 7.3.1 (Agilent Technologies, Santa Clara, CA, USA) data-mining software. Fold changes over 2.0 or under 0.5 and a p value <0.01 were considered to represent differential expression, and the significant genes in the BPH specimens were sorted by these criteria. The p values were calculated using Fisher's exact test.

In the gene ontology analysis, the scored gene lists were analyzed with the GO browser in Gene Spring[®] 7.3.1 (Bio Matrix Research, Chiba, Japan). In this analysis, in order to identify BPH-associated gene groups during growth, normal prostate was used as a control.

The functional network and pathway analyses were performed using GeneMAPP Pathways software, one of the functions of Gene Spring[®] 7.3.1 (Bio Matrix Research, Chiba, Japan). In this analysis, in order to identify BPH-specific gene groups during growth, both normal prostate and UGS were used as controls. Genes from the data set

were associated with cellular process, metabolic process, molecular function and physiological process in the GeneMAPP Pathways.

Real-time Quantitative RT-PCR

TaqMan PCR reagents for the 5 genes with the highest or lowest expression genes on the microarray were purchased from ABI (Applied Biosystems, CA), and applied according to the TaqMan Master Mix reagents kit protocol. The reactions were incubated for 2 min at 50°C, followed by denaturation for 10 min at 95°C. The reactions were run for 40 cycles of denaturation for 15 sec at 95°C, and an extension for 1 min at 60°C per cycle using a StepOne real-time PCR System (Applied Biosystems, CA). The data were standardized against beta-actin gene expression using Pre-Developed TaqMan Assay Reagents (Applied Biosystems, CA).

Results

Whole-genome oligonucleotide microarray analysis utilizing approximately 30,000 oligonucleotide probes was performed using normal prostate, non-transplanted UGSs

and transplanted UGSs (BPH specimens) during the process of growth of the prostate (21 days after implantation).

First, we compared the expression level between BPH specimens and normal prostate in order to identify genes associated with the process of growth of the prostate in BPH model rat. Microarray analyses revealed 926 up-regulated genes (>2 -fold change, $p < 0.01$) and 3,217 down-regulated genes (<0.5 -fold change, $p < 0.01$) in BPH specimens compared with normal prostate. Quantitative RT-PCR reconfirmed the expression level of the highest (>30 -fold change) or lowest expression genes (<0.1 -fold change) on the microarray, and validated that these genes significantly increased or decreased, respectively. (Table 1, Fig. 2).

We examined the expression of growth factor-, interleukin- and chemokine-related genes in BPH specimens because previous reports demonstrated that these genes were associated with the pathogenesis of BPH. As shown in Figure 3, some growth factor-related genes, interleukin-related genes and chemokine-related genes were significantly up-regulated in the BPH specimens compared with those in normal prostate specimens.

In order to examine the genes significantly associated with BPH, we categorized the up-regulated and down-regulated genes by gene ontology analysis. This analysis was performed utilizing the three categories of biological process, cellular components and molecular function using the 926 up-regulated and 3,217 down-regulated genes in BPH specimens compared with normal prostate (Fig. 4). In terms of biological process, up-regulated genes were predominantly involved in 3 of 11 categories: development (162 genes, $p=2.01 \times 10^{-4}$), response to stimulus (163 genes, $p=7.37 \times 10^{-13}$) and growth (32 genes, $p=1.93 \times 10^{-5}$). Genes associated with organ development and morphogenesis in the category of development, and genes associated with cell growth and regulation of growth in the category of growth were prominent in BPH specimens. Genes associated with response to biotic stimulus, response to external stimulus and response to stress were also prominent. In these categories, genes associated with defense response, response to external biotic stimulus, response to wounding, response to pathogen or parasite, and immune response were included. In the categories of cellular components and molecular function, no sorted categories were found. Down-regulated genes were not involved in any of the 11 categories.

When we compared the expression levels of BPH specimens with those of both normal prostate and non-transplanted UGSs, 507 up-regulated genes (>2 -fold change, $p < 0.01$) and 426 down-regulated genes (<0.5 -fold change, $p < 0.01$) were identified in BPH specimens. These genes were considered to represent the BPH-specific gene expression profile because they were obtained by removing genes commonly highly or lowly expressed in both BPH and UGS specimens from the analysis. We performed functional network and pathway analyses using GeneMAPP Pathways software in terms of which kinds of pathways the genes up-regulated and down-regulated in BPH specimens, are involved in (Fig. 5). The 507 up-regulated and 426 down-regulated genes were categorized into pathways associated with cellular process, metabolic process, molecular function and physiological process. Figure 4 shows the percentages of significantly up-regulated (>2 -fold change, $p < 0.01$) and down-regulated (<0.5 -fold change, $p < 0.01$) genes among the total genes examined in each pathway category of cellular process, metabolic process, molecular function and physiological process. The higher the percentage of significantly up-regulated or down-regulated genes among the total genes, the more the pathway was considered to be activated or inactivated,

respectively. Pathways in which over 15% of the total genes were up-regulated in BPH specimens were apoptosis modulation by heat shock protein 70, IL-1, -2 and -5 signaling pathway, and KIT signaling pathway in cellular process, and secretin-like G-protein-coupled receptors (GPCRs), Class B, in molecular process, suggesting that these pathways are relatively activated during the process of growth of the prostate in BPH specimens. On the other hand, pathways in which over 15% of the total genes were down-regulated in BPH specimens were cholesterol biosynthesis in metabolic process, suggesting that this pathway was relatively inactivated. Up-regulated and down-regulated genes in activated and inactivated pathways in BPH specimens are shown in Tables 2 and 3, respectively. In other pathways such as B-cell signaling pathway, p38 MAPK signaling pathway, eicosanoid synthesis, statin pathway, complement activation classical pathway, oxidative stress and protease degradation, a relatively large number of genes were up-regulated.

Discussion

Although several microarray studies have been conducted on human BPH tissues

[12,13], human BPH specimens were obtained from patients with advanced disease. Comparisons of genetic information between normal prostate and the BPH specimens during early growth have been limited in human study. In the present study, we performed microarray analysis using BPH model rats with both epithelial and stromal hyperplasia, resembling human BPH pathology, during prostate development, and compared the gene expression pattern between the normal prostate and BPH specimens in order to identify genes associated with the pathogenesis of BPH.

Although the development of BPH requires the presence of testicular androgens, androgens do not necessarily cause BPH. Recently, therefore, researchers have focused on the androgen-independent pathway. Previous reports demonstrated that multiple families of growth factors, cytokines and chemokines act through paracrine signaling to stimulate proliferation [14-16]. In our microarray study using the BPH model, genes associated with growth factors, cytokines and chemokines were up-regulated in the BPH specimens compared with those in normal prostate, suggesting that this model could be suitable as a BPH rat model to elucidate the androgen-independent molecular and cellular mechanism involved in BPH.

Our microarray analyses revealed 926 up-regulated genes and 3,217 down-regulated genes in BPH specimens compared with those in normal prostate. We categorized the up- and down-regulated genes by gene ontology analysis. In the category of biological process, the up-regulated genes were subcategorized into 3 groups: development, response to stimulus and growth, in the BPH specimens. Since we examined the difference of gene expression between normal prostate and BPH specimens during the growth process, the up-regulation of genes associated with development and growth was to be expected. A noteworthy finding here is the up-regulation of genes associated with response to stimulus, including genes associated with response to biotic stimulus, external stimulus and stress. The presence of inflammatory cells infiltrating the prostate stroma and epithelium is an extremely common finding in human BPH specimens [17-19]. Inflammation may serve as the trigger for BPH by a chronic state of wound repair and tissue regeneration. Our genetic observations demonstrated that the genes associated with defense and immune response, and response to external biotic stimulus, wounding and pathogens could be activated in this BPH model, suggesting that external biotic stimulus and pathogens induce inflammation in the prostate and trigger prostatic

growth in aging human males.

A wide range of signaling factors expressed in the UGS are expressed in the BPH as well, lending support to the concept that developmental growth pathways are reactivated in the adult prostate [20]. In our study, by removing genes commonly highly expressed or lowly expressed in both BPH and UGS specimens from the analysis, 507 up-regulated genes and 426 down-regulated genes were identified, which were considered to represent the BPH-specific gene expression profile. These BPH-specific genes may be associated with BPH-specific growth. Using these genes, therefore, we performed functional network and pathway analyses to categorize the BPH-specific genes and detect the BPH-specific growth mechanism. We demonstrated a direct functional link between BPH pathogenesis and BPH-specific signaling pathways in the BPH model rat.

As described above, the complex proinflammatory microenvironment is closely related to prostatic hyper-proliferation [17-20]. Prostatic inflammation observed in BPH may cause the release of some kinds of cytokines from inflammatory cells. These cytokines released from inflammatory cells may not only interact with immune effectors but also

with prostatic stromal and epithelial cells [20-24]. Inflammatory mediators may contribute to prostatic epithelial and stromal cell growth both directly, through the induction of growth via cytokines that stimulate the production of prostatic growth factors, and indirectly through decreases in prostate cell death via the down-regulation of prostate cell apoptosis [22,25]. Our functional network and pathway analyses showed that some interleukin signaling pathways were activated in BPH specimens. As described above, some interleukin-related genes were up-regulated in the BPH specimens compared with normal prostate specimens. Therefore, our findings suggest that these cytokines elicit changes in downstream signaling pathways and in the tissue microenvironment during BPH development in the BPH model.

Our functional network and pathway analyses also suggested that the KIT receptor signaling pathway and cholesterol biosynthesis were associated with BPH pathogenesis. Previous reports have already shown the association of these pathways with the pathogenesis of BPH, and KIT regulated cell proliferation in the prostate plays a significant role in the pathophysiology of BPH [26]. The prostate synthesizes and stores a large amount of cholesterol, and prostate tissue is sensitive to changes in cholesterol

metabolism [27].

We also found that novel pathways, including apoptosis modulation by heat shock protein 70 and secretin-like GPCRs, Class B, were likely to be associated with the development and growth of the prostate in the BPH model. In addition, some genes in other pathways, such as B-cell signaling pathway, p38 MAPK signaling pathway, eicosanoid synthesis, statin pathway, complement activation classical pathway, oxidative stress and protease degradation were up-regulated. There is a possibility that these pathways have a strong correlation with BPH pathogenesis.

In our study, molecular profiling and classification of the BPH model identified some candidate genes and pathways associated with BPH pathogenesis. Further characterization of the genes and pathways obtained from the microarray analyses may identify the genes responsible for BPH and clarify their complex relationship, as well as promote the development of molecular-targeted agents for molecules responsible for this condition.

Acknowledgements

This work was supported in part by research grants from the Scientific Fund of the Japan Health Science Foundation, 26462448 from the Japanese Ministry of Education, Culture, Science and Technology, The Takeda Science Foundation, The Nakatomi Foundation and The Uehara Memorial Foundation.

Conflict of interest

None declared.

References:

1. Lawson RK. Role of growth factors in benign prostatic hyperplasia. *Eur. Urol.* 1997;**32**:22-27.
2. McVary KT. BPH: epidemiology and comorbidities. *Am. J. Manag. Care* 2006;**12**:S122-128.
3. Shapiro E, Becich MJ, Hartanto V, Lepor H. The relative proportion of stromal and epithelial hyperplasia is related to the development of symptomatic benign prostate hyperplasia. *J. Urol.* 1992;**147**:1293-1297.
4. Golomb E, Rosenzweig N, Eilam R, Abramovici A. Spontaneous hyperplasia of the ventral lobe of the prostate in aging genetically hypertensive rats. *J. Androl.* 2000;**21**:58-64.
5. Scolnik MD, Servadio C, Abramovici A. Comparative study of experimentally induced benign and atypical hyperplasia in the ventral prostate of different rat strains. *J. Androl.* 1994;**15**:287-297.
6. Mori F, Oda N, Sakuragi M, Sakakibara F, Kiniwa M, Miyoshi K. New histopathological experimental model for benign prostatic hyperplasia: stromal hyperplasia in rats. *J. Urol.* 2009;**181**:890-898.
7. Matityahou A, Rosenzweig N, Golomb E. Rapid proliferation of prostatic epithelial cells in spontaneously hypertensive rats: a model of spontaneous hypertension and prostate hyperplasia. *J. Androl.* 2003;**24**:263-269.
8. Yamashita M, Zhang X, Shiraishi T, Uetsuki H, Kakehi Y. Determination of percent

- area density of epithelial and stromal components in development of prostatic hyperplasia in spontaneously hypertensive rats. *Urology*. 2003;**61**:484-489.
9. Kojima Y, Sasaki S, Oda N, *et al*. Prostate growth inhibition by subtype-selective alpha(1)-adrenoceptor antagonist naftopidil in benign prostatic hyperplasia. *Prostate* 2009;**69**:1521-1528.
 10. Kojima Y, Sasaki S, Kubota Y, *et al*. Up-regulation of α 1a and α 1d-adrenoceptors in the prostate by administration of subtype selective α 1-adrenoceptor antagonist tamsulosin in patients with benign prostatic hyperplasia. *J. Urol.* 2011;**186**:1530-1536.
 11. Bosch RJ. Pathogenesis of benign prostatic hyperplasia. *Eur. Urol.* 1991;**20**:27-30.
 12. Prakash K, Pirozzi G, Elashoff M, *et al*. Symptomatic and asymptomatic benign prostatic hyperplasia: molecular differentiation by using microarrays. *Proc. Natl. Acad. Sci. U S A.* 2002;**99**:7598-603.
 13. Luo J, Dunn T, Ewing C, *et al*. Gene expression signature of benign prostatic hyperplasia revealed by cDNA microarray analysis. *Prostate* 2002;**51**:189-200.
 14. Lee KL1, Peehl DM. Molecular and cellular pathogenesis of benign prostatic hyperplasia. *J. Urol.* 2004;**172**:1784-1791.
 15. Bechis SK, Otsetov AG, Ge R, Olumi AF. Personalized medicine for the management of benign prostatic hyperplasia. *J. Urol.* 2014;**192**:16-23.
 16. Macoska JA. Chemokines and BPH/LUTS. *Differentiation*. 2011;**82**:253-60.
 17. Delongchamps NB, de la Roza G, Chandan V, *et al*. Evaluation of prostatitis in autopsied prostates--is chronic inflammation more associated with benign prostatic

- hyperplasia or cancer? *J. Urol.* 2008;**179**:1736-1740.
18. Nickel JC, Roehrborn CG, O'Leary MP, Bostwick DG, Somerville MC, Rittmaster RS. The relationship between prostate inflammation and lower urinary tract symptoms: examination of baseline data from the REDUCE trial. *Eur. Urol.* 2008;**54**:1379-1384.
 19. Robert G, Descazeaud A, Nicolaiew N, *et al.* Inflammation in benign prostatic hyperplasia: a 282 patients' immunohistochemical analysis. *Prostate.* 2009;**69**:1774-1780.
 20. McLaren ID, Jerde TJ, Bushman W. Role of interleukins, IGF and stem cells in BPH. *Differentiation* 2011;**82**:237-243.
 21. Fibbi B, Penna G, Morelli A, Adorini L, Maggi M. Chronic inflammation in the pathogenesis of benign prostatic hyperplasia. *Int. J. Androl.* 2010;**33**:475-488.
 22. Bostanci Y, Kazzazi A, Momtahn S, Laze J, Djavan B. Correlation between benign prostatic hyperplasia and inflammation. *Curr. Opin. Urol.* 2013;**23**:5-10.
 23. Briganti A, Capitanio U, Suardi N, *et al.* Benign prostatic hyperplasia and its aetiologies. *Eur. Urol. Suppl.* 2009; **8**:865–871.
 24. Robert G, Descazeaud A, Allory Y, Vacherota F, de la Taille A. Should we investigate prostatic inflammation for the management of benign prostatic hyperplasia? *Eur. Urol. Suppl.* 2009; **8**:879–886.
 25. St Sauver JL, Jacobsen SJ. Inflammatory mechanisms associated with prostatic inflammation and lower urinary tract symptoms. *Curr. Prostate. Rep.* 2008; **6**:67–73
 26. Imura M, Kojima Y, Kubota Y, *et al.* Regulation of cell proliferation through a

KIT-mediated mechanism in benign prostatic hyperplasia. *Prostate*.
2012;**72**:1506-1513.

27. Freeman MR, Solomon KR. Cholesterol and benign prostate disease. *Differentiation*.
2011;**82**:244-252.

Figure Legends

Figure 1. Histological findings of normal adult prostate (A,B,C), urogenital sinus before implantation (D,E,F) and BPH (G,H,I). In the BPH specimen, the proportion of the stromal components with smooth muscle and extracellular matrix was increased. In addition, the presence of inflammatory cells infiltrating the prostate stroma was found.

Hematoxylin and eosin stain. A,D,G: x100. B,E,H: x200. C,F,I: x200.

Figure 2. Quantitative RT-PCR on the highest (A; >30-fold change) or lowest (B; <0.1-fold change) expression genes extracted from microarray analysis. n=4 per group, *p<0.05, **p<0.01

Figure 3. Average fold change of growth factor- (A), interleukin- (B) and chemokine-related genes (C) in BPH. *: p<0.01

Figure 4. Gene ontology analyses using 926 up-regulated and 3,217 down-regulated genes in BPH samples compared with normal prostate. Number in parentheses each are the number of genes in each category.

Figure 5. Percentage of significantly up-regulated (A, C, E, G) and down-regulated (B, D, F, H) genes among the total genes examined in each pathway of cellular process (A,

B), metabolic process (C, D), molecular function (E, F) and physiological process (G, H).

Figure

Figure 1.

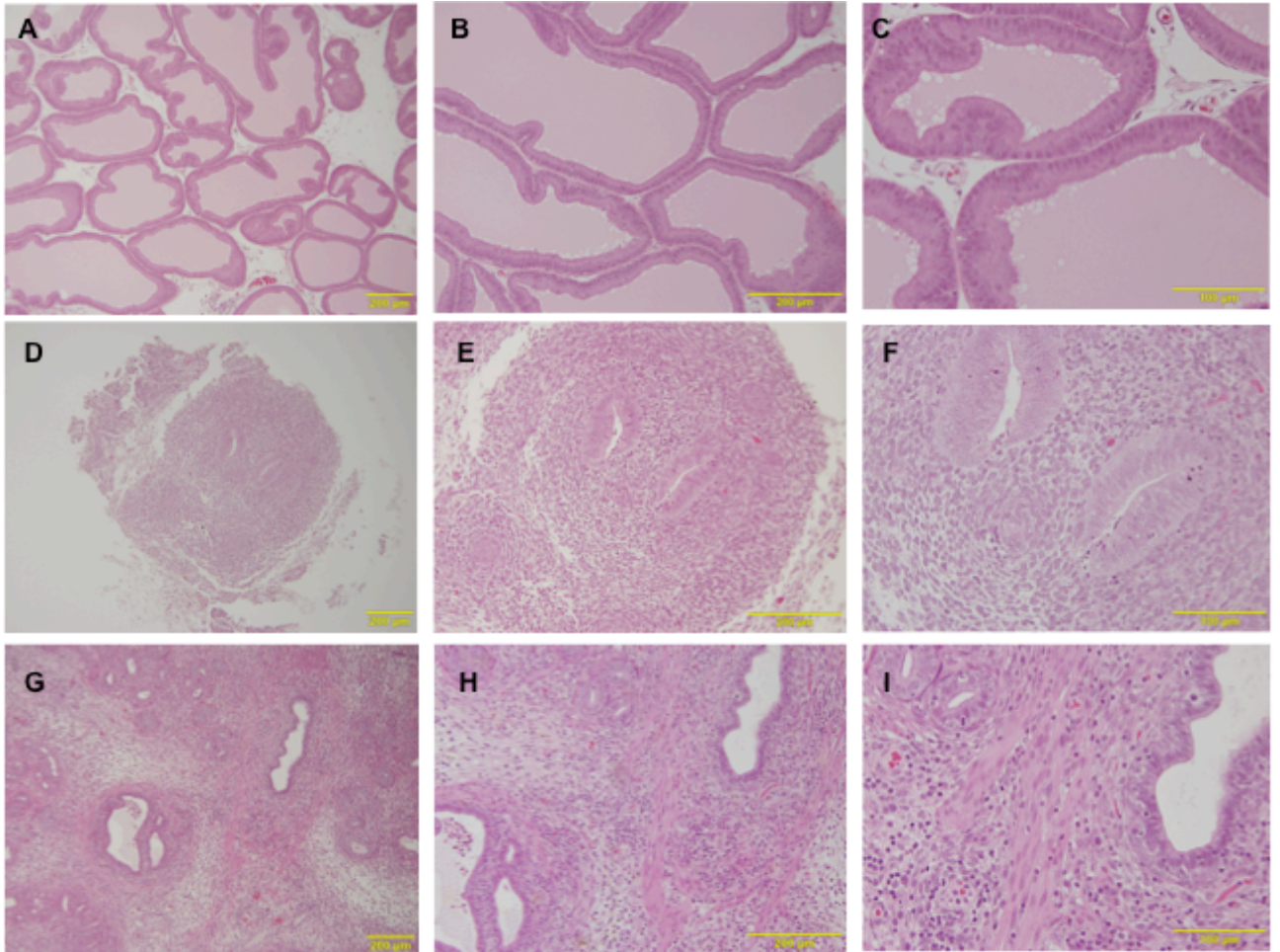
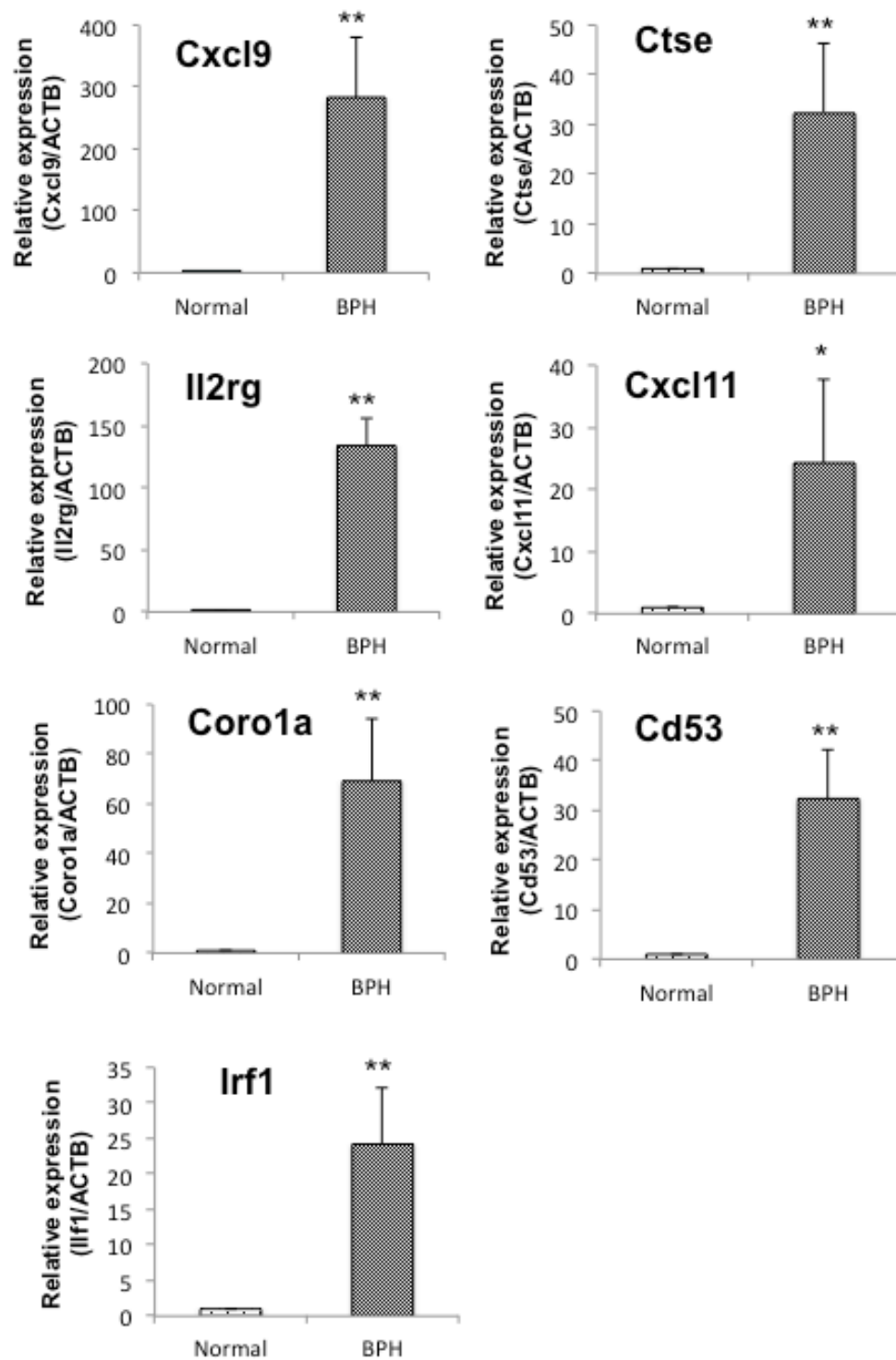
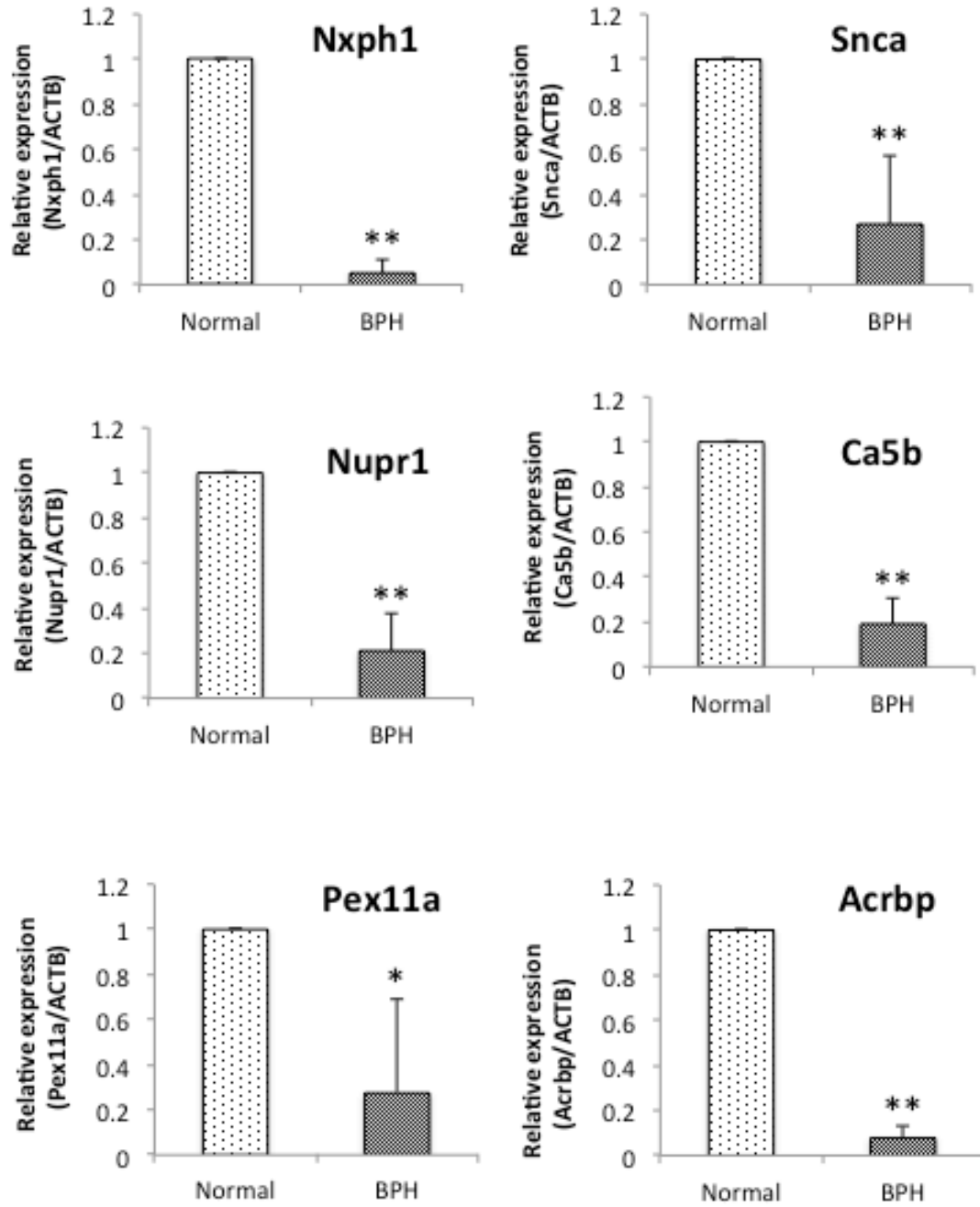


Figure 2.

A



B



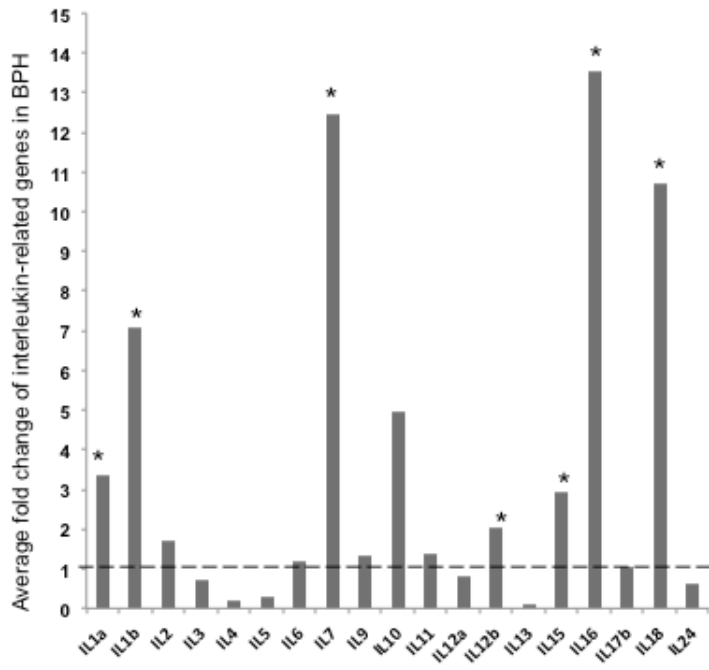
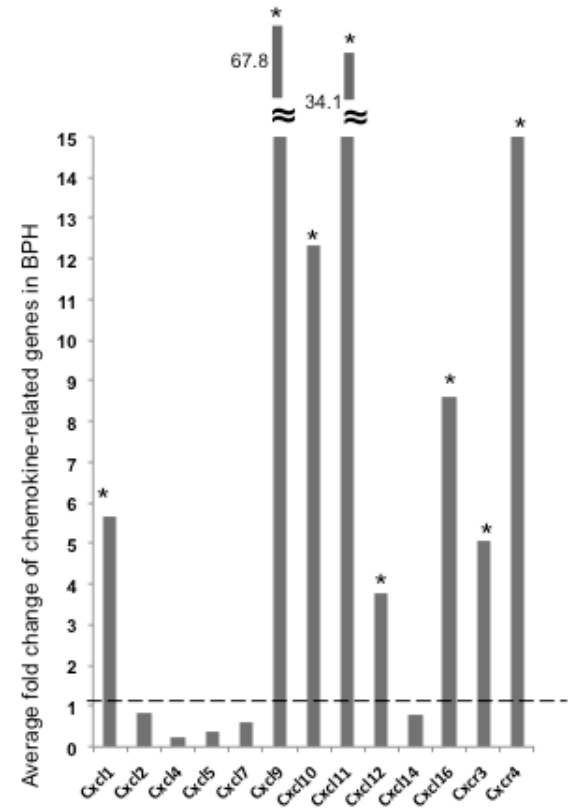
B**C**

Figure 4.

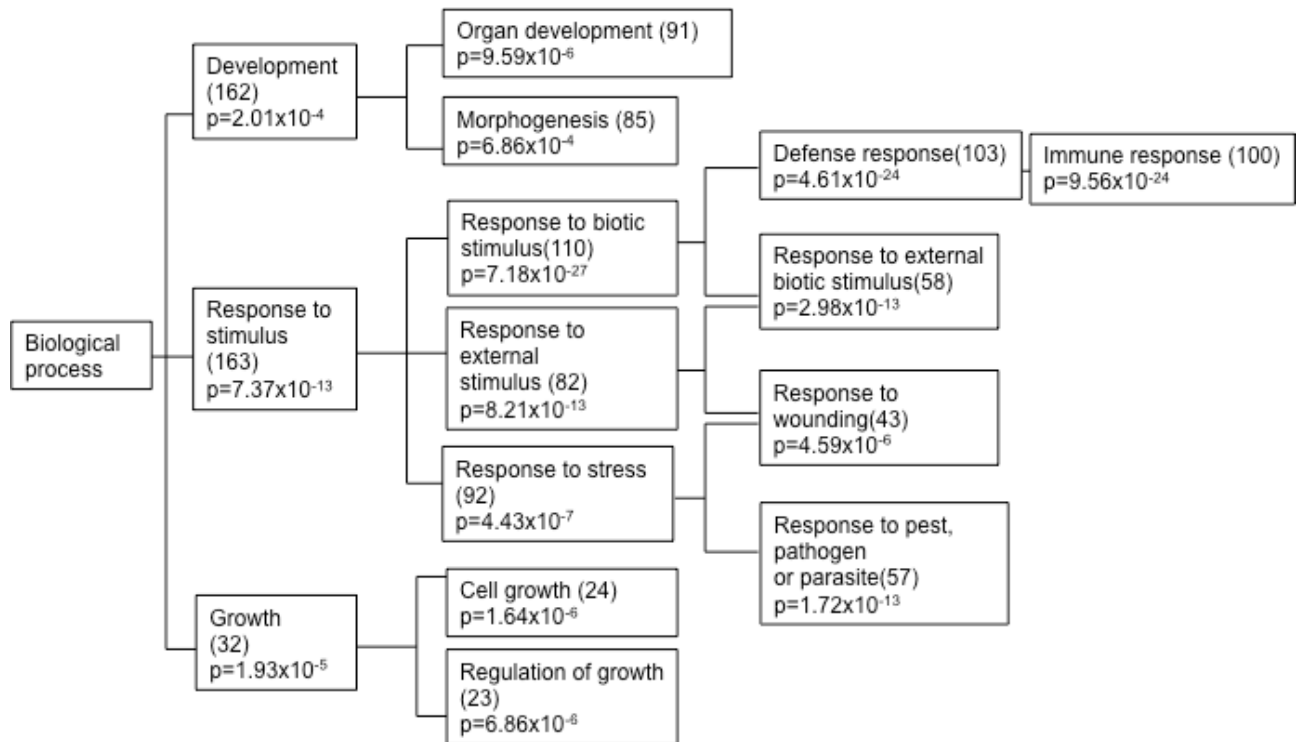
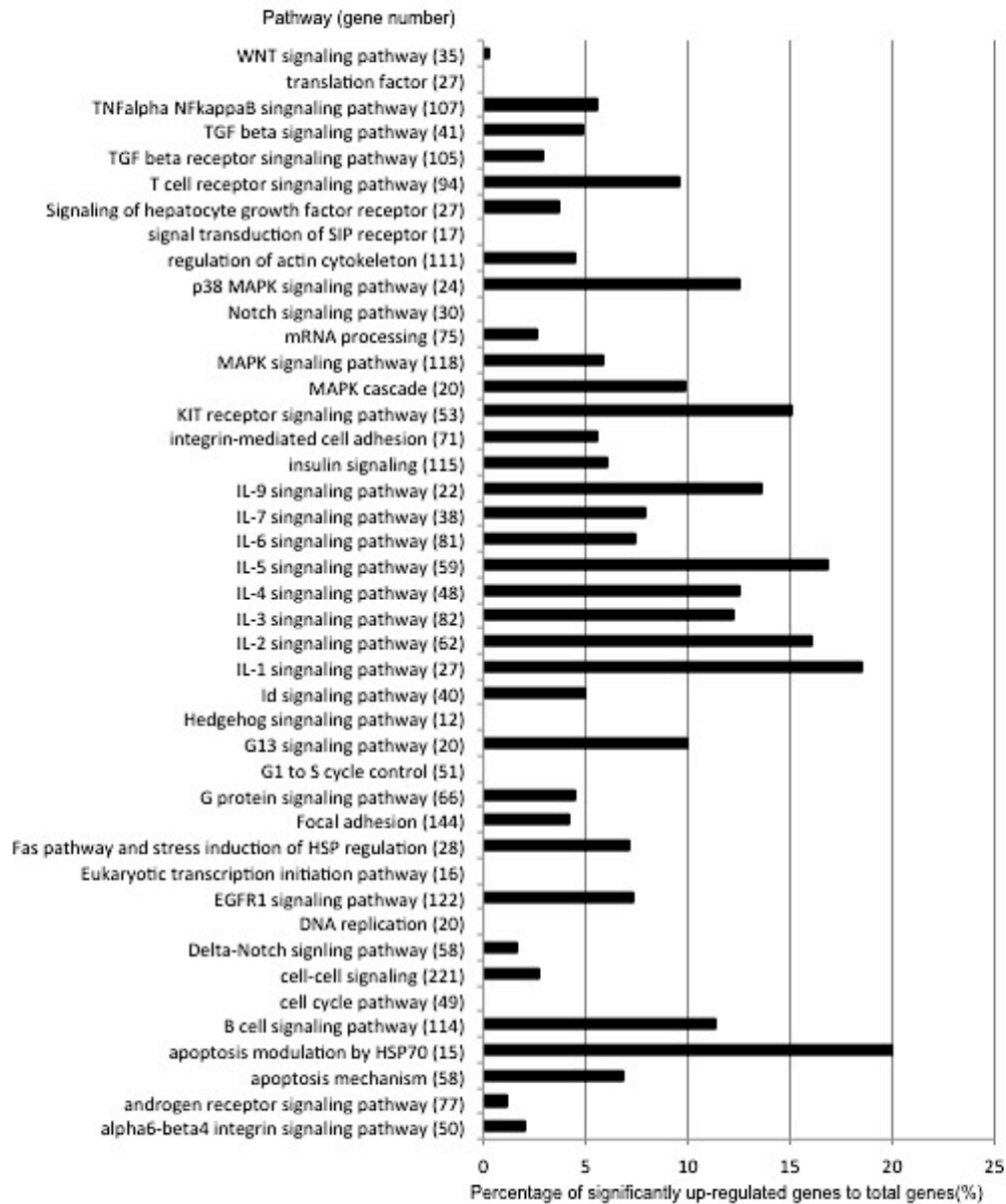
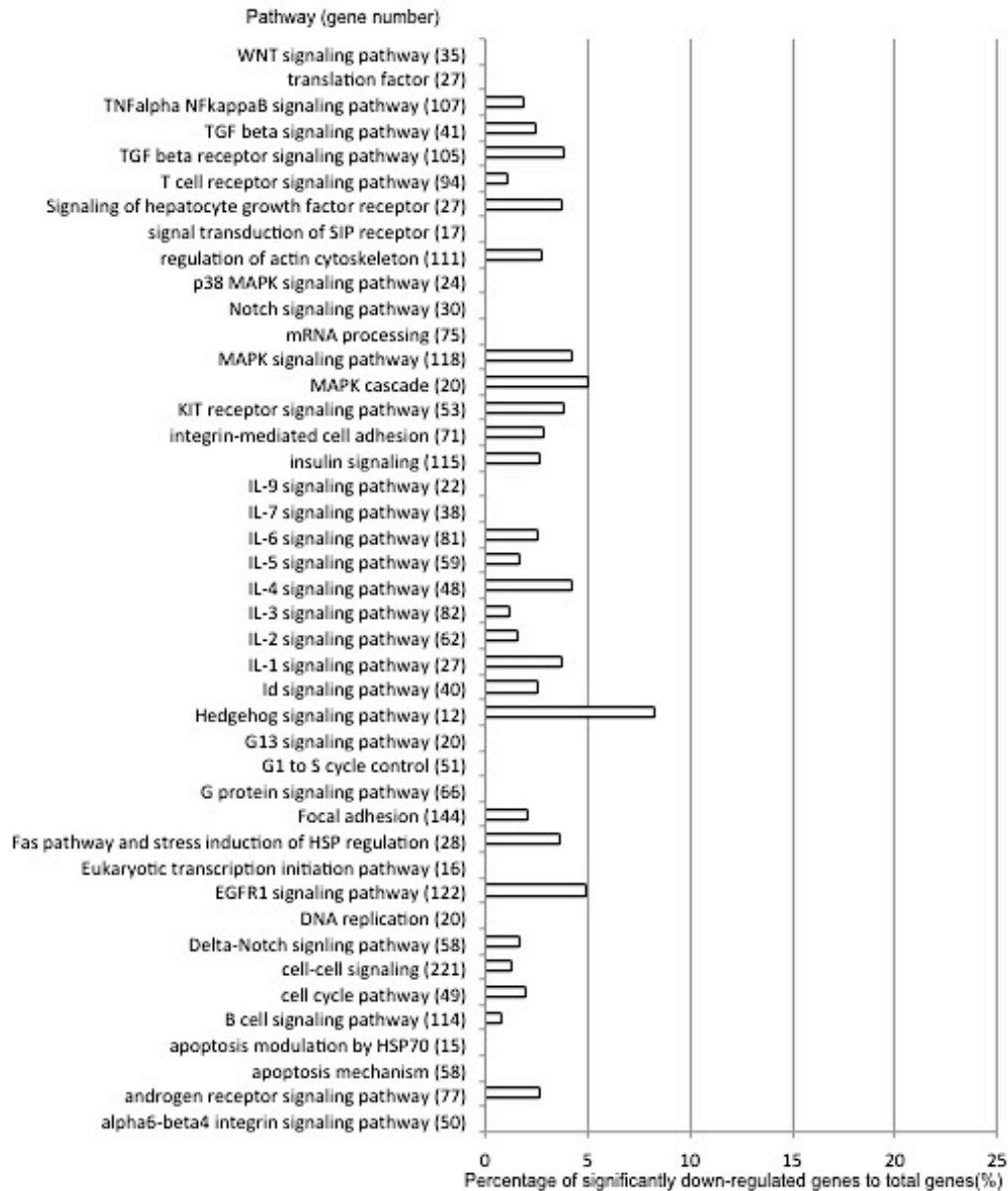


Figure 5.

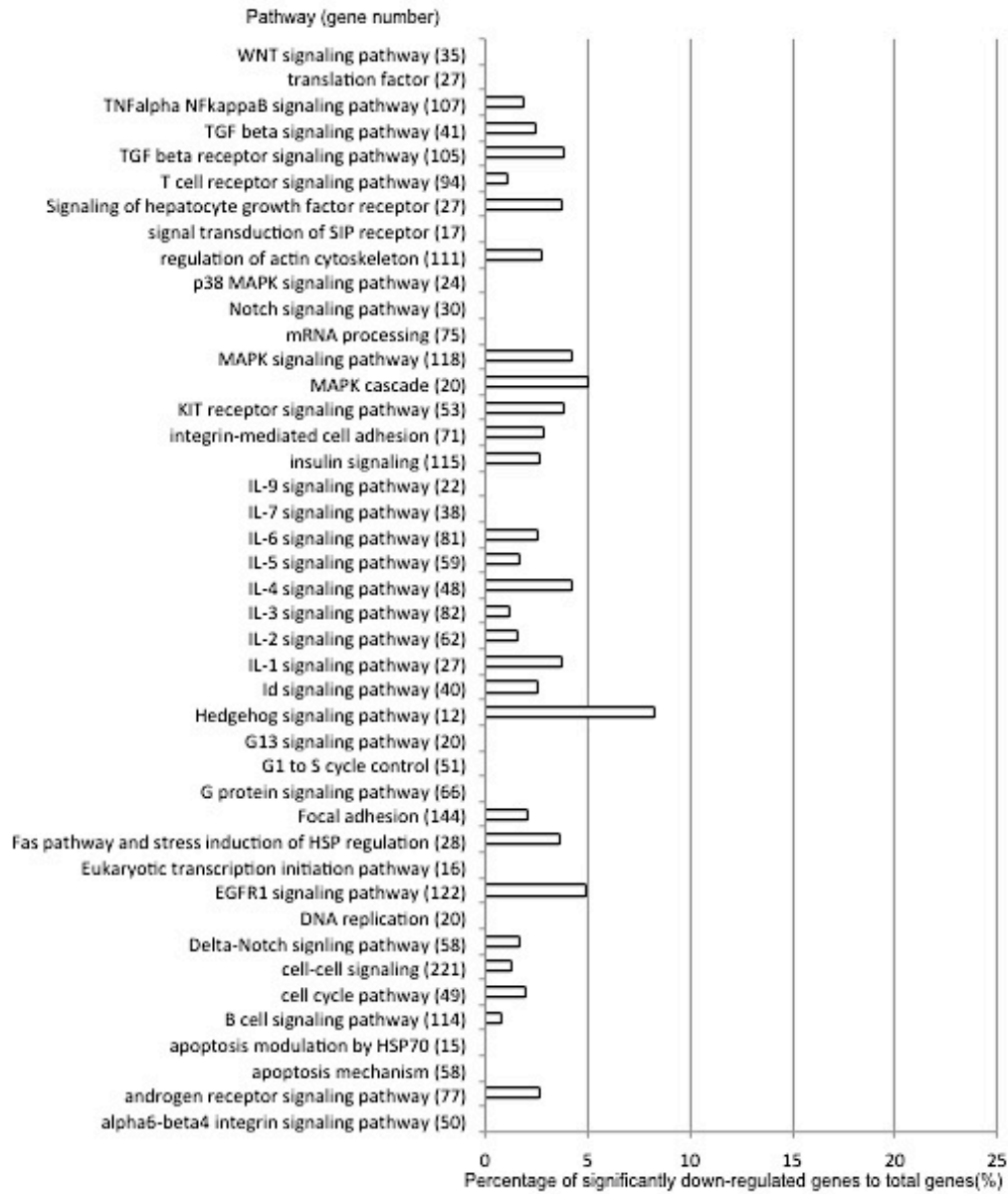
A



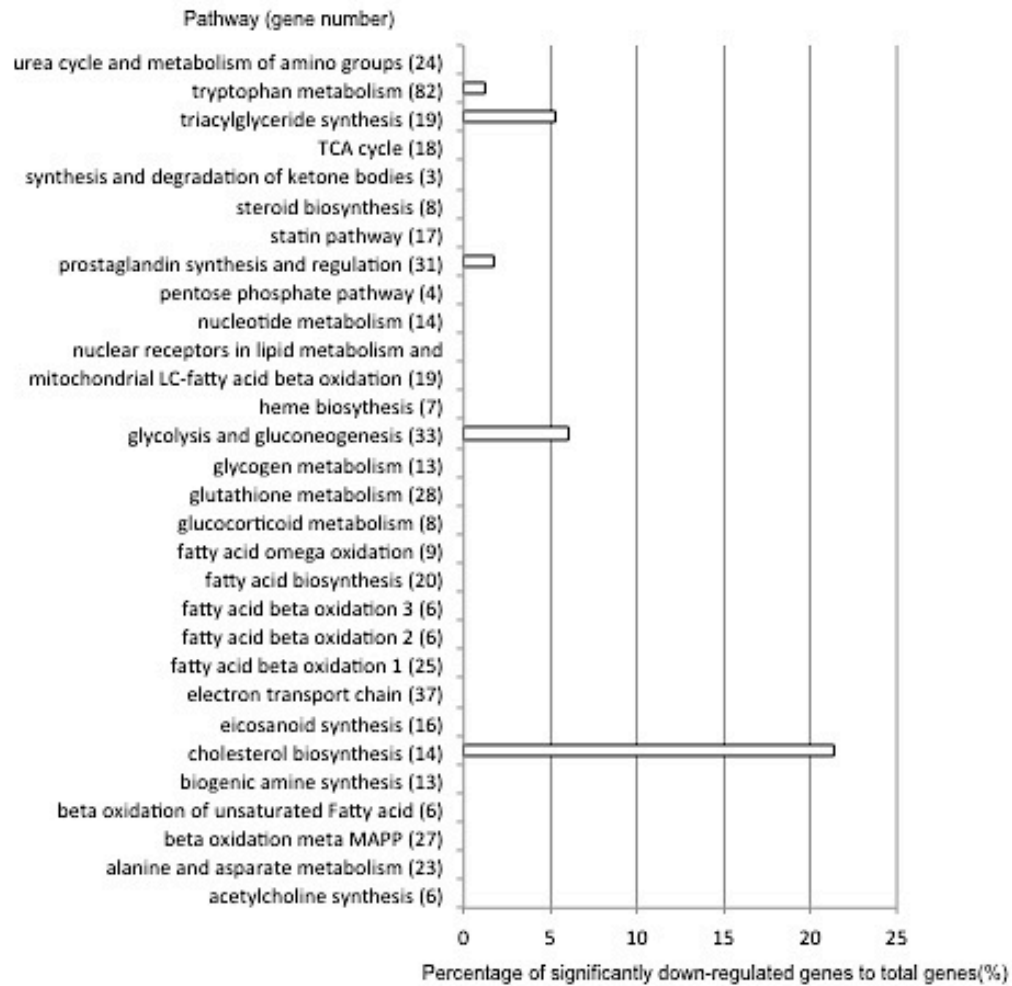
B



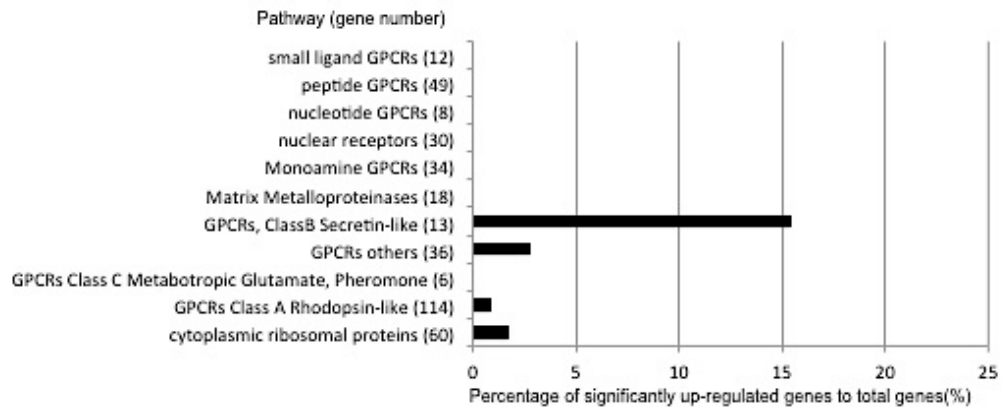
C



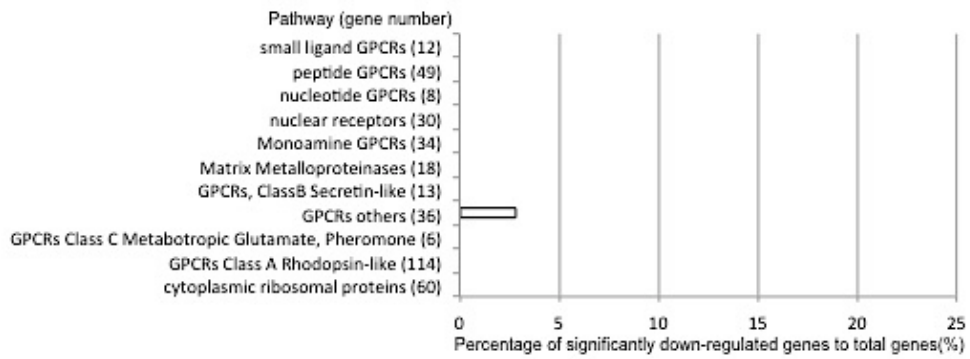
D



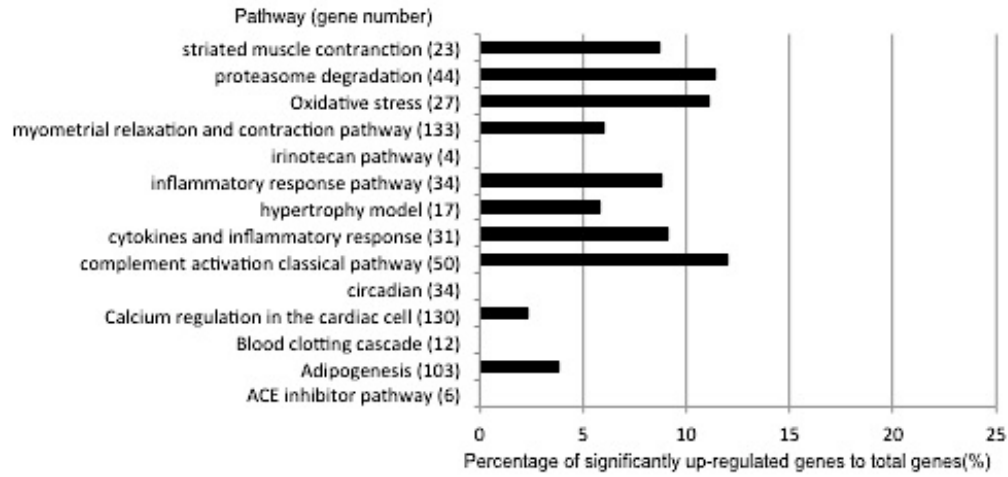
E



F



G



H

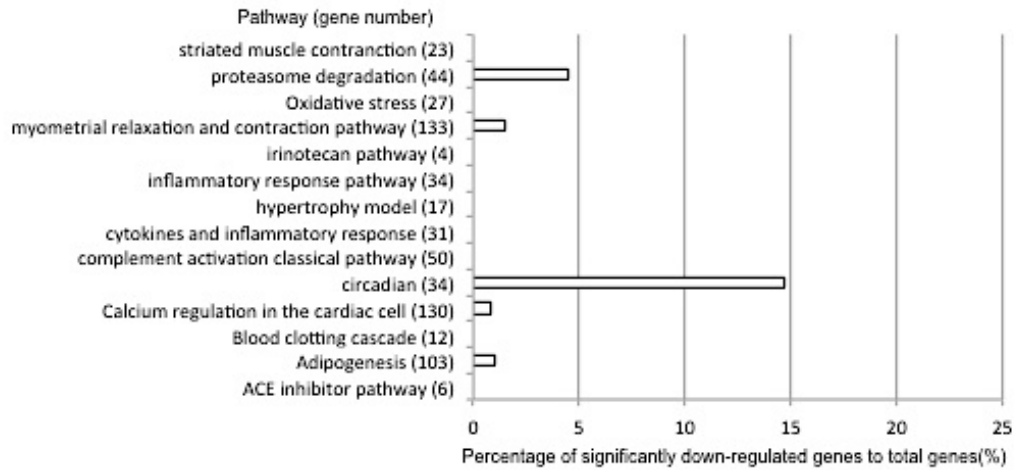


Table 1.

Table 1. Highest or lowest expression genes in BPH model on the microarray

| Systematic | Gene Symbol | Description | Genbank | Average fold change (Min to Max) | t-test P-value |
|------------|----------------|-----------------------------------|-----------|-------------------------------------|-----------------------|
| 1373544_at | Cxcl9 | chemokine (C-X-C motif) ligand 9 | AI170387 | 67.77 (20.14 to 125.7) | 1.61x10 ⁻³ |
| 1368167_at | Ctse | cathepsin E | NM_012938 | 36.84 (24.83 to 72.14) | 2.85x10 ⁻³ |
| 1389092_at | Il2rg | interleukin 2 receptor, gamma | AI178808 | 36.55 (26.04 to 53.34) | 2.60x10 ⁻⁴ |
| 1379365_at | Cxcl11 | chemokine (C-X-C motif) ligand 11 | BF281987 | 34.05 (12.44 to 61.67) | 1.35x10 ⁻³ |
| 1369964_at | Coro1a | coronin, actin binding protein 1A | NM_130411 | 32.26 (25.02 to 38.37) | 5.73x10 ⁻⁵ |
| 1368518_at | Cd53 | CD53 antigen | NM_012523 | 31.73 (28.58 to 37.08) | 5.85x10 ⁻⁴ |
| 1368073_at | Irf1 | interferon regulatory factor 1 | NM_012591 | 30.49 (14.8 to 54.22) | 8.33x10 ⁻³ |

| Systematic | Gene Symbol | Description | Genbank | Average fold change (Min to Max) | t-test P-value |
|--------------|----------------|--------------------------------------|-----------|-------------------------------------|-----------------------|
| 1385799_at | Nxph1 | neurexophilin 1 | AW531533 | 0.0288 (0.01 to 0.0974) | 3.81x10 ⁻² |
| 1367977_at | Snca | synuclein, alpha | NM_019169 | 0.0731 (0.0358 to 0.145) | 1.08x10 ⁻² |
| 1367847_at | Nupr1 | nuclear protein 1 | NM_053611 | 0.0784 (0.0328 to 0.183) | 2.06x10 ⁻² |
| 1377573_at | Ca5b | carbonic anhydrase VB, mitochondrial | AI411132 | 0.0877 (0.0421 to 0.162) | 4.17x10 ⁻² |
| 1398552_a_at | Acrbp | acrosin binding protein | BG381450 | 0.0917 (0.0394 to 0.181) | 2.72x10 ⁻² |
| 1387740_at | Pex11a | peroxisomal biogenesis factor 11A | NM_053487 | 0.0946 (0.0455 to 0.209) | 5.45x10 ⁻³ |

Table 2.

Table 2. Up-regulated genes in activated pathway in BPH specimens

| Category | systematic | Gene Symbol | Description | GenBank | Average fold change (Min to Max) | p-value |
|--------------------------------|--------------|-------------|--|-----------|----------------------------------|-----------------------|
| Apoptosis modulation by HSP70 | 1389170_at | Casp7 | caspase 7 | BF283754 | 2.14 (1.72 to 2.95) | 3.94x10 ⁻³ |
| | 1370968_at | Nfkb1 | nuclear factor of kappa light chain gene enhancer in B-cells 1, p105 | AA858801 | 2.24 (1.78 to 2.71) | 2.28x10 ⁻⁴ |
| | 1368871_at | Map3k1 | mitogen activated protein kinase kinase kinase 1 | NM_053887 | 2.20 (1.97 to 2.41) | 7.59x10 ⁻⁵ |
| IL-1 signaling pathway | 1374468_at | Myd88 | myeloid differentiation primary response gene 88 | AI236590 | 2.18 (1.69 to 3.05) | 6.86x10 ⁻³ |
| | 1383474_at | Irak2 | interleukin-1 receptor-associated kinase 2 | BI274988 | 2.59 (1.63 to 3.36) | 6.55x10 ⁻³ |
| | 1367881_at | Ptpns1 | protein tyrosine phosphatase, non-receptor type substrate 1 | NM_013016 | 2.72 (1.62 to 4.36) | 9.61x10 ⁻⁴ |
| | 1370968_at | Nfkb1 | nuclear factor of kappa light chain gene enhancer in B cells 1, p105 | AA858801 | 2.24 (1.78 to 2.71) | 2.28x10 ⁻⁴ |
| | 1369186_at | Casp1 | caspase 1 | D85899 | 15.54 (7.57 to 29.84) | 2.03x10 ⁻⁴ |
| IL-2 signaling pathway | 1368856_at | Jak2 | Janus kinase 2 | NM_031514 | 2.18 (1.51 to 2.82) | 5.86x10 ⁻³ |
| | 1368010_at | Ptpn6 | protein tyrosine phosphatase, non-receptor type 6 | NM_053908 | 3.61 (2.47 to 5.43) | 4.85x10 ⁻³ |
| | 1368186_a_at | Syk | spleen tyrosine kinase | U21683 | 3.57 (2.82 to 5.55) | 1.06x10 ⁻³ |
| | 1368231_at | Stat5a | signal transducer and activator of transcription 5A | NM_017064 | 2.88 (2.07 to 3.85) | 9.94x10 ⁻⁴ |
| | 1381875_at | Nmi | N-myc (and STAT) interactor | BM386847 | 4.86 (3.32 to 7.30) | 2.83x10 ⁻⁴ |
| | 1370968_at | Nfkb1 | nuclear factor of kappa light chain gene enhancer in B cells 1, p105 | AA858801 | 2.24 (1.78 to 2.71) | 2.28x10 ⁻⁴ |
| | 1372757_at | Stat1 | signal transducer and activator of transcription 1 | BM386875 | 8.91 (5.35 to 12.76) | 6.28x10 ⁻⁵ |
| | 1368518_at | Cd53 | CD53 antigen | NM_012523 | 29.36 (18.52 to 48.12) | 3.12x10 ⁻⁵ |
| | 1391171_at | Itn2b | Integral membrane protein 2B | AW534352 | 2.92 (2.50 to 3.61) | 1.81x10 ⁻⁵ |
| | 1389092_at | Il2rg | interleukin 2 receptor, gamma | AI178808 | 34.70 (24.72 to 50.64) | 9.64x10 ⁻⁷ |
| IL-5 signaling pathway | 1387566_at | Pla2g4a | phospholipase A2, group IVA (cytosolic, calcium-dependent) | NM_133551 | 2.78 (2.47 to 5.43) | 9.39x10 ⁻³ |
| | 1368856_at | Jak2 | Janus kinase 2 | NM_031514 | 2.18 (1.51 to 2.82) | 5.86x10 ⁻³ |
| | 1368010_at | Ptpn6 | protein tyrosine phosphatase, non-receptor type 6 | NM_053908 | 3.61 (2.47 to 5.43) | 4.85x10 ⁻³ |
| | 1368186_a_at | Syk | spleen tyrosine kinase | U21683 | 3.57 (2.82 to 5.55) | 1.06x10 ⁻³ |
| | 1368231_at | Stat5a | signal transducer and activator of transcription 5A | NM_017064 | 2.88 (2.07 to 3.85) | 9.94x10 ⁻⁴ |
| | 1369204_at | Hck | hemopoietic cell kinase | NM_013185 | 19.04 (8.69 to 38.33) | 3.52x10 ⁻⁴ |
| | 1370261_at | Rps6ka1 | ribosomal protein S6 kinase polypeptide 1 | BI285433 | 2.59 (2.19 to 2.78) | 2.63x10 ⁻⁴ |
| | 1370585_a_at | Prkcb1 | protein kinase C, beta 1 | X04440 | 5.16 (3.66 to 8.12) | 2.52x10 ⁻⁴ |
| | 1370968_at | Nfkb1 | nuclear factor of kappa light chain gene enhancer in B cells 1, p105 | AA858801 | 2.24 (1.78 to 2.71) | 2.28x10 ⁻⁴ |
| | 1372757_at | Stat1 | signal transducer and activator of transcription 1 | BM386875 | 8.91 (5.35 to 12.76) | 6.28x10 ⁻⁵ |
| KIT receptor signaling pathway | 1368856_at | Jak2 | Janus kinase 2 | NM_031514 | 2.18 (1.51 to 2.82) | 5.86x10 ⁻³ |
| | 1368010_at | Ptpn6 | protein tyrosine phosphatase, non-receptor type 6 | NM_053908 | 3.61 (2.47 to 5.43) | 4.85x10 ⁻³ |
| | 1368231_at | Stat5a | signal transducer and activator of transcription 5A | NM_017064 | 2.88 (2.07 to 3.85) | 9.94x10 ⁻⁴ |
| | 1369204_at | Hck | hemopoietic cell kinase | NM_013185 | 19.04 (8.69 to 38.33) | 3.52x10 ⁻⁴ |
| | 1370261_at | Rps6ka1 | ribosomal protein S6 kinase polypeptide 1 | BI285433 | 2.59 (2.19 to 2.78) | 2.63x10 ⁻⁴ |
| | 1387198_at | Inpp5d | inositol polyphosphate-5-phosphatase D | NM_019311 | 7.36 (5.52 to 12.19) | 1.39x10 ⁻⁴ |
| | 1372757_at | Stat1 | signal transducer and activator of transcription 1 | BM386875 | 8.91 (5.35 to 12.76) | 6.28x10 ⁻⁵ |
| GPCRs, Class B Secretin-like | 1381311_at | Emr1 | EGF-like module containing, mucin-like, hormone receptor-like sequence 1 | BE100625 | 19.83 (7.04 to 60.29) | 4.87x10 ⁻³ |
| | 1372468_at | Cd97 | CD97 antigen | BI296525 | 3.87 (2.61 to 6.14) | 5.27x10 ⁻⁴ |

Table 3.

Table 3. Down-regulated genes in inactivated pathway in BPH specimens

| Category | systematic | Gene Symbol | Description | GenBank | Average fold change (Min to Max) | p-value |
|--------------------------|------------|-------------|---|-----------|----------------------------------|-----------------------|
| cholesterol biosynthesis | 1387020_at | Cyp51 | cytochrome P450, subfamily 51 | BG664123 | 0.34 (0.25 to 0.56) | 9.43x10 ⁻³ |
| | 1387017_at | Sqle | squalene epoxidase | NM_017136 | 0.38 (0.26 to 0.54) | 6.49x10 ⁻³ |
| | 1368878_at | Idi1 | isopentenyl-diphosphate delta isomerase | NM_053539 | 0.34 (0.26 to 0.50) | 3.69x10 ⁻³ |